Cover Page

Fill out and attach to your manuscript — DUE Thursday, December 1, 2011

International Toki Conference (ITC-21)

Integration of Fusion Science and Technology For Steady State Operation

Abstract Number:	**1003**
Registration Number:	**0007**
Paper Title:	**Recent TCV results – innovative plasma shaping to improve plasma properties and insight**
Corresponding Author:	**Antoine POCHELON**
Affiliation:	**Ecole Polytechnique Fédérale de Lausanne (EPFL), Centre de Recherches en Physique des Plasmas, Association Euratom-Confédération Suisse**
Full Postal Address:	**EPFL, SB, CRPP, Building PPB, Station 13, CH-1015 Lausanne, Switzerland**
Telephone:	**(+41 21) 693 34 38**
Fax:	**(+41 21) 693 51 76**
E-mail:	**Antoine.Pochelon@epfl.ch**
Topic Category:	**1**

LIST OF TOPICS

1. Progress in fusion plasma confinement
2. Plasma-wall interactions and divertor technology
3. Materials and blankets
4. Superconducting magnets, cryogenic systems and related technologies
5. Heating and fueling
6. Plasma diagnostics and control
7. Safety, environment and tritium control
8. Modeling and simulation for fusion plasma
9. Concepts of steady state DEMO
10. Interdisciplinary issues between fusion and other fields

Recent TCV results – innovative plasma shaping to improve plasma properties and insight

A. Pochelon, P. Angelino, R. Behn, S. Brunner, N. Kirneva[1], S.Yu. Medvedev[2], H. Reimerdes, J. Rossel, O. Sauter, L. Villard, D. Wagner, A. Bottino[3], Y. Camenen[4], G.P. Canal, P.K. Chattopadhyay[5], S. Coda, B.P. Duval, T.P. Goodman, S. Jolliet, A. Karpushov, B. Labit, A. Marinoni, J-M. Moret,
A. Pitzschke, L. Porte, M. Rancic, V.S. Udintsev[6] and the TCV Team.

Ecole Polytechnique Fédérale de Lausanne (EPFL), Centre de Recherches en Physique des Plasmas, Associations Euratom-Confédération Suisse, CH-1015 Lausanne, Switzerland

[1]*NRC-Kurchatov Institute, Kurchatov Sq. 1, 123182 Moscow, Russia*

[2]*Keldysh Institute, Russian Academy of Sciences, Miusskaya Sq. 4, 125047 Moscow, Russia*

[3]*Max-Planck Institut für Plasmaphysik, IPP-Euratom Association, Garching bei München, Germany*

[4]*International Institute for Fusion Science, University of Provence, Marseille, France*

[5]*Institut for Plasma Physics, Bhat, Gandhinagar, Gujarat, India*

[6]*ITER Organisation, St Paul lez Durance, France*

The TCV tokamak facility is used to study the effect of innovative plasma shapes on core and edge confinement properties. In low collisionality L-mode plasmas with electron cyclotron heating (ECH) confinement increases with increasingly negative triangularity δ. The confinement improvement correlates with a decrease of the inner core electron heat transport, even though triangularity vanishes to the core, pointing to the effect of global – non-local – transport properties. TCV has recently started the study of the effects of negative triangularity in H-mode plasmas. H-mode confinement is known to improve towards positive triangularity, due to the increase of pedestal height, though plagued by large edge localised modes (ELMs). An optimum triangularity could thus be sought between steep edge barriers (δ>0) with large ELMs, and improved core confinement (δ<0) with small ELMs. This opens the possibility for a reactor of having H-mode-level confinement within an L-mode edge, or at least with mitigated ELMs. In TCV, ELMy H-modes with δ_{top}<0 are explored, showing a reduction of ELM peak energy losses. Alternative shapes are proposed in the light of ideal MHD stability calculations. Shaping has the potential to bring at the same time key solutions to confinement, stability and wall loading issues and, from the comparison of experimental and simulation results, to give deeper insight in gyrokinetic and stability modelling.

Keywords: confinement, plasma shape, triangularity, global transport, gyrokinetic simulations, H-mode, ELMs.

1. Introduction

Confinement and stability are central issues of magnetic plasma confinement, since high energy confinement time and plasma pressure are key ingredients of an economical reactor. In a tokamak reactor, instabilities relaxing power pulses can lead to severe or non-tolerable erosion of the first wall. Plasma shaping, by influencing both confinement and stability properties, can be used as a free parameter in the optimization of the design of a reactor, ahead of ITER.

Apart from enhancing performances, there are other solid motivations justifying to study plasma shapes further than ITER shapes. Shaping is an excellent tool for the test and validation of plasma modelling, e.g. transport and stability. Also, the usual confinement τ_E-scaling laws exhibit no triangularity dependence, but confinement in TCV plasma core improves towards negative triangularity δ<0 in low collisional L-mode discharges when in the trapped electron mode (TEM) turbulence regime – a regime probable to occur in reactor conditions. In contrast, it is well established from different tokamak H-

mode studies that both the pedestal heights - and ELM sizes - increase as δ increases, and thus confinement increases with triangularity in the positive triangularity domain. It is therefore of high interest to explore the properties of H-modes at negative δ to investigate pedestal properties and assess the ELM behaviour.

Our long-term objective is then the optimization of the plasma triangularity aiming at both the maximization of core confinement and the mitigation of ELMs, or whether both can be simultaneously achieved in a reactor.

The paper is constructed as follows. The introduction describes different effects of plasma shape on confinement and stability, focalizing on triangularity. The improved confinement and transport obtained at negative triangularity in low collisionality TEM is summarized in section 2 and compared with local and global gyrokinetic modelling in section 3, which stresses the relevance of global properties. The exploration of the new domain of H-mode at negative triangularity is the subject of section 4, followed in section 5 by the MHD stability analysis relevant to the H-mode experiments developed, and prospects gained from these calculations.

2. Confinement and transport improvement towards negative triangularity (δ<0)

The TCV tokamak facility [FH94] (R=0.88m, a=0.25m, R/a~3.5, B≤1.5T, I_p≤1MA) offers extreme shaping flexibility with its 16 independent poloidal field coils, which allowed to achieve: elongation 0.9<κ<2.8, triangularity - 0.7<δ<1, varied squareness, SN, DN, and snowflake divertor. This flexibility in shape is matched by a flexible ECH system [TPG08]: 4.5 MW at 2nd (X2) and 3rd (X3) harmonic with 7 independent launchers enabling local power deposition for any plasma shape.

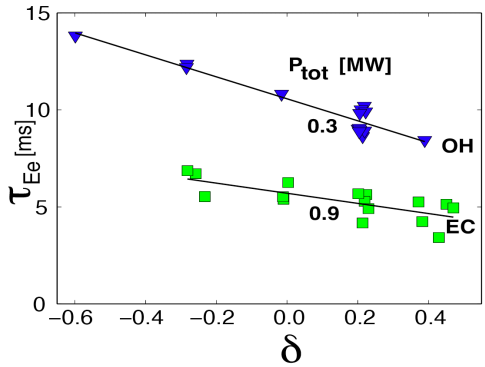

Fig.2.1 Confinement time as a function of triangularity for two different powers in low collisionality plasmas [Pochelon99].

Energy confinement was found to improve towards δ<0 in low-density EC heated L-mode plasmas, Fig.2.1 [Pochelon99], a result in surprising contrast to earlier results in medium density Ohmic plasmas, where no effect of triangularity was observed [Moret97]. The ECH plasma conditions in which the effect was found are: low-density ECH plasmas, high R/L_{Te}>7 and T_e/T_i~3-5, that is in the TEM dominated regime and in the low collisionality domain ν_{eff}~0.2-1, later identified as being the vital parameter [Camenen05].

Local heat deposition with ECH enabled exhaustive local heat transport measurements at mid-radius, over a wide range of electron temperature T_e and electron temperature gradients R/L_{Te}, which allowed isolating collisionality ν_{eff} as a key element. The heat diffusivity χ_e increases with triangularity and decreases with ν_{eff}; the heat diffusivity is typically reduced by a factor 2 with negative triangularity δ over a wide range of collisionality ν_{eff}<1, Fig.2.2 [Camenen07]. This means also that to sustain at negative triangularity δ=-0.4 a pressure profile identical to the one at δ=0.4 requires only half of the power [Camenen07]. It follows from the same experiments that χ_e is halved *over all radia* outside the heat deposition location, here located just outside the q=1 radius at ρ_v~0.3 (see e.g. Fig.6 in [Marinoni09]).

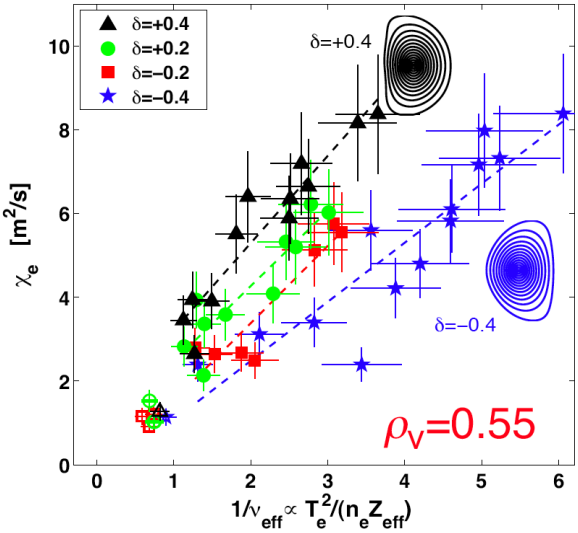

Fig.2.2 Radial energy transport measured at mid-radius for a scan of positive and negative triangularities at different collisionalities, $\chi_e(1/\nu_{eff})$ [Camenen07].

A new way of demonstrating the effect of triangularity on transport deep inside the plasma is to measure the confinement response to a radial sweep of constant power deposition. This is shown in Fig.2.3, where the improvement factor over the standard L-mode,

H_{RLW}, is shown as a function of the radius of power deposition [Kirneva12]. The resulting confinement is fair for power deposition close to plasma axis, particularly inside q=1, and lowering as the deposition moves to the edge, as known. Meaningful in this context, the H-factor is substantially higher at negative triangularity (δ=-0.4) compared to positive (δ=+0.4), and the beneficial effect on confinement subsists and is effective deep in the core.

Surprisingly, the strong variation of transport with δ is not limited to the edge region, as for the "geometric" triangularity, which decays quickly from the edge (δ at mid-radius represents 25% of edge value). This is a direct evidence of the presence of global effects in TEM transport, revealed here by plasma shaping.

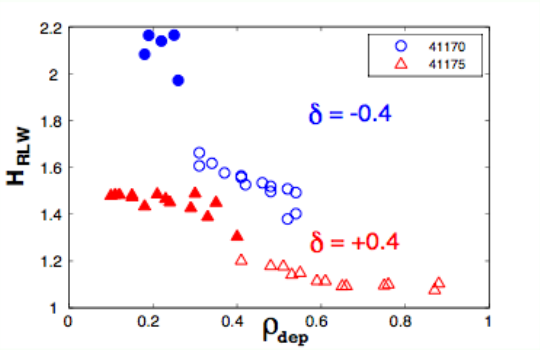

Fig.2.3 Dependence of the confinement factor H_{RLW} in a sweep of radial EC-power deposition for a negative and a positive triangularity δ discharge, showing improved confinement at negative δ at all deposition radia, including at the very core. Open symbols: deposition outside the q=1 region, and solid, inside.

3. Comparison with transport models – global transport effects

Local GK simulations: *Local (flux-tube)* gyrokinetic simulations with the GS2 code first in the *linear* mode show that most of the mixing length TEM transport occurs in the range $k_\theta \rho_i \sim 0.3$. This is also the range mostly affected by triangularity changes. The mixing length estimate of the heat diffusivity decreases towards δ<0, thus indicating the same trend as in the experiment [Marinoni09]. Note that all the simulations are based on actual TCV equilibria.

Non-linear flux-tube estimates of χ_e can also be calculated with GS2, e.g. at different radial depth. The ratio $\chi_e(d=+0.4)/\chi_e(d=-0.4)$, and particularly its radial dependence, is a measure of the change of transport with triangularity, of the penetration of triangularity effects. The triangularity effect on χ_e is found to vanish rapidly towards the centre in this local gyrokinetic calculation, in fact as rapidly as the local geometric triangularity decreases. This stands in contrast to the experimental χ_e from power balance, for which the triangularity effect on χ_e is nearly constant with radius, that is indeed penetrates.

The non-linear flux-tube – local – GS2 calculations predict correctly χ_e to decrease with increasing collisionality ν_{eff}, when trying to reproduce the behaviour of Fig.2.2., but a correct difference due to triangularity can only be found in the periphery and at the lowest collisionalities, in despairing contrast to experiment.

The difficulties arise along the radial coordinate: the experiment is demanding a stronger radial link mediating transport between core and edge, calling for so-called global transport.

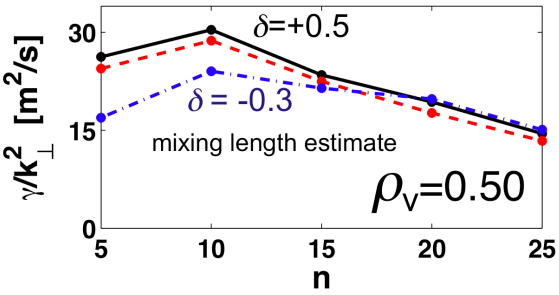

Fig.3.1 Mixing length estimate from ORB5 showing reduction of energy transport at negative triangularity, predominantly for the low toroidal mode number n (triangularity δ = -0.3, +0.2, +0.5).

Global GK simulations: *Global transport* effects are expected for finite but not too small values of $\rho^* = \rho_L/a$. In TCV, ρ^*~1/70, thus finite ρ^* effects are expected, i.e. differences between local and global simulation. This means that global simulations are required to account for the full radial profiles. Here, the global gyrokinetic code ORB5 [JollietCPC07] enables to carry out linear and non-linear, collisional simulations. In this paper, to evaluate the present effect of triangularity on transport, linear runs have been carried out so far, here also using actual TCV equilibria [Camenen05].

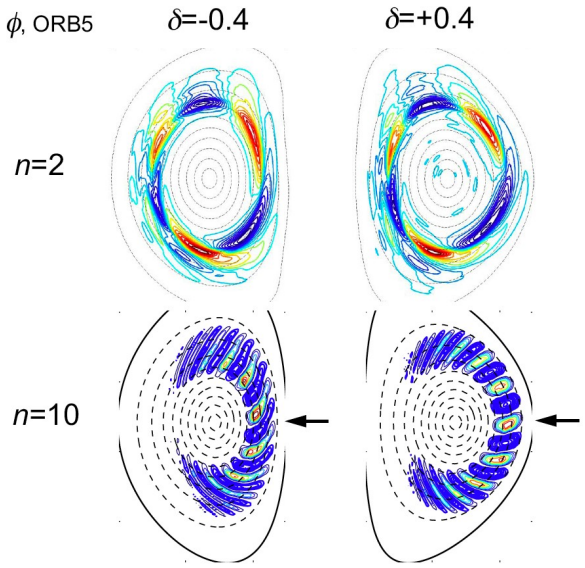

Fig.3.2 Poloidal plot of the potential for transport relevant low n TEM showing large radial extension and visible reduction (arrow) in the perpendicular wavelength for n=2, 10.

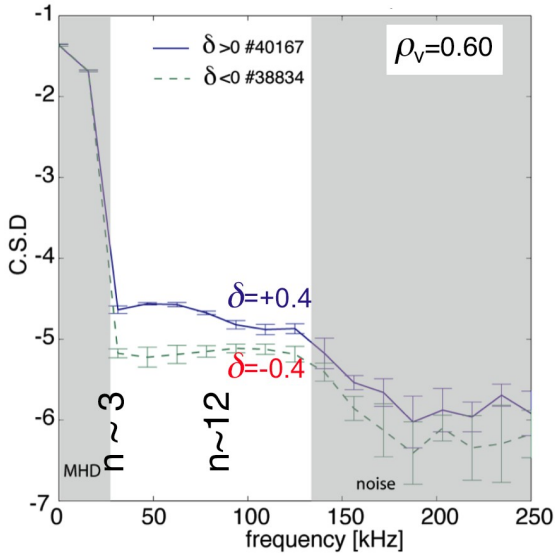

Fig.3.3 Electron temperature fluctuations at positive and negative triangularity from correlation-ECE measured at the same flux surface, showing an amplitude reduction at the low frequencies with negative triangularity.

Evaluating the effect of triangularity on the mixing length transport, similar frequencies and growth rates are found as a function of the toroidal wave number n. The main change with triangularity is the perpendicular wave vector $k_\perp$. Therefore, the mixing length transport estimate at mid-radius is reduced at δ<0, essentially through the reduction of $k_\perp$ of the TEM predominantly at the low n's [Camenen07], see Fig.3.1. Linear global runs are relevant, since saturation mechanisms like zonal flows play limited role in the case of TEMs [JollietThès09].

A plot of the instability potential φ in the poloidal plane of typical low n modes is shown in Fig.3.2. It shows 1) the *large radial extension* of the modes see e.g. n=2, and 2) the *reduction in radial wavelength at* δ<0, particularly visible in the mid plane LFS for n=10.

These typical mode numbers n are relevant to experimental turbulence, in particular in the sense that they are found to delimit more or less the frequency band in which the T_e-fluctuations are modified by triangularity, see Fig.3.3.

In fact, the electron temperature fluctuations from correlation ECE diagnostics have been measured in the discharge mid-plane at mid-radius on the LFS. Going from δ=+0.4 to δ=-0.4, a systematic reduction of the fluctuation amplitude was found for the first time, of the order of a factor 2 in the range $30 < f < 80$ kHz (corresponding to $3 < n < 12$) and measured at a radius of ρ_v=0.6 [LabitFEC10]. Due to the larger Shafranov shift at negative triangularity, care was taken to measure the turbulence on the same magnetic flux surface, the variation of Shafranov shift being typically $\Delta\rho$~0.1. Neglecting this shift results in a larger apparent reduction, due to the decrease with radius of a factor 2 per $\Delta\rho$~0.10 at this location [PochelonAPS10]. Since plasma rotation is essentially unchanged for both triangularities δ=±0.4 [SauterFEC10], the reduction of fluctuation amplitude observed does not originate from a Doppler effect.

Therefore, the frequency domain where turbulence is modified by triangularity corresponds to low-n modes range ($3<n<12$) i.e. modes of large radial extension.

This leads us to raise the issue whether the confinement beneficial effect of negative triangularity found in L-mode could be extended to H-mode. But H-mode at negative triangularity is unexplored.

4. H-mode properties at negative triangularity – ELM mitigation

ELM behaviour. Reliable H-mode operation at negative triangularity was developed recently in centred

single null (SNC) discharges. This plasma geometry - with the EC resonance major radius close to the X-point - provides adequate accessibility to the 2nd harmonic (X2) electron cyclotron resonance for edge plasma heating, even with overdense central densities, see Fig.4.1a left. Robust, 99% first pass X2 absorption inside the separatrix, with $P_{in}>>P_{thres}$ (typically 1.5-2.5 times above H-mode threshold) enables control over the ELM regime. X2 power, 300-900kW, are deposited at a location close to the edge, ρ_{dep}=0.9, unchanged during the triangularity sweep, see Fig.4.1 right. X3 power is launched from the top with a poloidal angle that has been optimized to follow the shape change. Typically 500-700kW X3 power are absorbed close to the core. Different EC power P_{EC} waveforms have been explored. The typical plasma parameters are: elongation κ=1.7, triangularity δ_{top}=+0.2 to -0.2, q_{95} = 2.3, $n_{e\ av}$~3.5 10^{19} m^{-3}, ´ ÑB towards X-point.

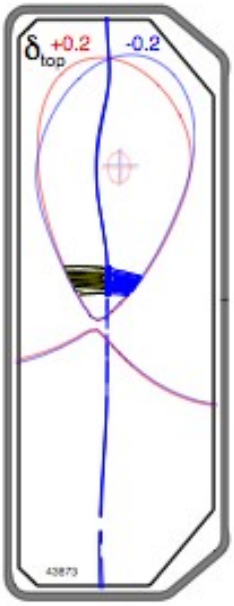

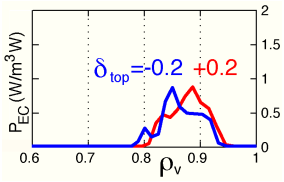

Fig.4.1
Left: Single Null Centred (SNC) equilibrium of the triangularity, swept from δ_{top}=+0.2 to -0.2, together with the X2 heating beam path used to control the H-mode regime. The cold resonance quasi-aligned with the X-point provides good X2 access. (Fig/Ant/ .eps)

Bottom: X2 power deposition location maintained constant throughout shape sweep.

The triangularity dependence of H-mode properties and ELM behaviour has been studied by continuously sweeping the upper triangularity in the range $-0.2<\delta_{top}<+0.2$, as indicated in Fig.4.1. For both positive and negative triangularity, the ELM frequency f_{ELM} increases with increasing total power ($P_{tot} = P_{X2}+P_{X3}+P_{\Omega}$), which identifies type I ELMs, as shown in Fig.4.2. This enables us to study high-power H-mode operation as a function of triangularity and type I ELM regime - the ELM regime that will cause excessive erosion of the plasma-facing components in a reactor, if not mitigated.

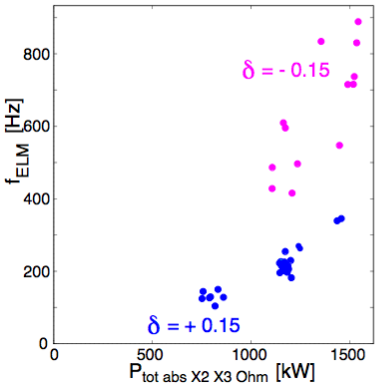

Fig.4.2 Power dependence of ELM frequency: f_{ELM} increases with power for positive and negative triangularity.

The **ELM amplitude** is found to decrease towards δ<0, as seen from D_α emission and the diamagnetic loop [Moret03], $\Delta W_{ELM}/W$, while the ELM frequency increases. Over the range δ_{top}= +0.2 to -0.2, negative triangularity brings a 3-fold increase in f_{ELM}, and a 3-fold reduction of peak losses $\Delta W_{ELM}/W$, as shown in Fig.4.3.

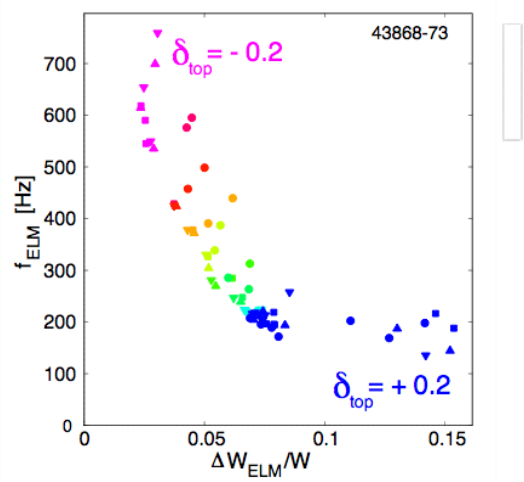

Fig.4.3 Type I ELM amplitude and frequency for different triangularity δ_{top}. Towards negative triangularity, the ELM frequency increases and the relative ELM energy loss decreases, both by a factor of 3 over the range δ_{top}=+0.2 to -0.2. The colours represent equal size classes of triangularities.

Throughout the triangularity scan, care was taken to fix the **location** of X2 power **deposition**. This is important, since it was observed recently that f_{ELM} increases with the deposition location moving to the edge [RosselThes12] in similar discharges. In the current δ_{top}-scan, X2 power deposition location was maintained constant at typically ρ_{dep}=0.9 (ρ_v!). If there is any displacement, it is by less than 1% inwards (ρ_v), which validates that the triangularity ELM frequency behaviour

is genuine and does not originate from an unintentional displacement of the power deposition location. It was noticed that the effect of the centrally deposited X3 power on f_{ELM} is substantially smaller than that of edge deposited X2 power, which confirms and extends Rossel's results.

Confinement analysis in H-mode. After having successfully decreased the ELM energy loss by reducing triangularity towards negative values, there is concern about determining the specific contributions of core transport and edge barrier to the confinement as a function of triangularity. Obviously, the predominant edge-heating scheme, due to the cut-off, used for ELM control is not optimal for confinement studies.

With a dominant fraction of power deposited close to the edge, these discharges are optimized for the control and study of H-mode and ELM properties, but are not optimal for aiming confinement studies. The densities, or more crucially the collisionalities, are higher than in the earlier L-mode experiments, which showed an improved confinement at δ<0 [Camenen07].

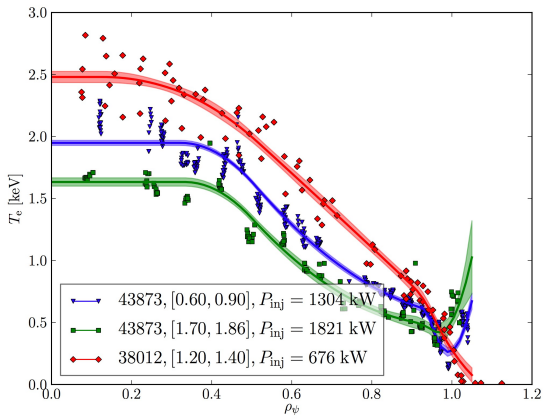

Fig.4.4 Electron pressure profile for positive and negative triangularity (δ_{top}= ±0.2), showing the reduction in pedestal height towards negative triangularity. (indicative Fig.!: Better show p_e, and with the "cleaned" Thomson data by Roland).

A preliminary analysis of the confinement regime yields: collisionality ν_{eff}~1 measured at ρ_ν~0.5 ($\nu_{eff} \approx 0.1 R Z_{eff} n_e / T_e$, where lengths are in m, densities in 10^{19} m^{-3}, temperatures in keV, see [Angioni03]), R/L_n=2-3, R/L_{Te}=10 but low R/L_{Ti}. The GS2 transport code indicates TEM dominated regime for both triangularities δ_{top}= ±0.2.

From δ_{top}= +0.2 to -0.2, the pressure pedestal height decreases by ~30%. Fig.4.4 Show T_e and n_e profiles at δ_{top}= ±0.2. (not only the pedestal profile, but the full profiles, with DW profile fits). The energy confinement time τ_E normalized to TCV scaling ($\tau_E / n_e^{0.46} P^{-0.7}$) [Pochelon99] shows similar 30% decrease.

Consequently, in these H-mode studies, the edge barrier is responsible for the essential of the confinement change with δ_{top}. In fact with a collisionality ν_{eff}~1 in the present TCV H-mode at δ_{top}=±0.2, confinement improvement towards δ_{top}<0 should not be expected from past experience on core transport reduction towards δ_{top}<0 [Camenen07, Fig.6]. In order to take advantage of the confinement improvement at negative triangularity, the collisionality of the H-modes has to be reduced. In TCV, the density cannot be lowered, since it is already close to the H-mode low-density limit. Higher temperature with supplementary core electron heating (X3, O2) is required at theses H-mode densities to benefit of core confinement improvement δ<0. In a reactor, this condition can be realized at reactor electron temperatures with central electron α-heating.

5. H-mode stability, δ-scan and outlook

The ideal MHD stability analysis of the above triangularity scan, which has demonstrated the reduction of the ELM energy loss, is presented in this section. In addition, possible ways of improving edge stability of negative triangularity plasmas in terms of pressure limits are described, exploring different shapes including X-point(s) or snowflake divertor located on the LFS.

The KINX code was developed for ideal stability calculations in presence of an X-point [Degtyarev97]. The effect of snowflake divertor was analyzed recently [MedvedevCPP10]. The case of negative triangularity and the influence of the major radius of the X-point were specifically studied in preparation of the experiments presented here [MedvedevEPS11].

KINX calculations for equilibria with SNC and with increasingly δ_{top}<0 show that the *n*-infinity ballooning mode limit moves gradually to smaller pressure gradients, see Fig.5.1, closing the access to 2nd stability region. Here the stability maps are presented as functions of the normalized parallel current density $J_\parallel/\langle J\rangle$ and normalized pressure gradient α taken at the position of maximal pressure gradient in the pedestal as in [MedvedevCPP10].

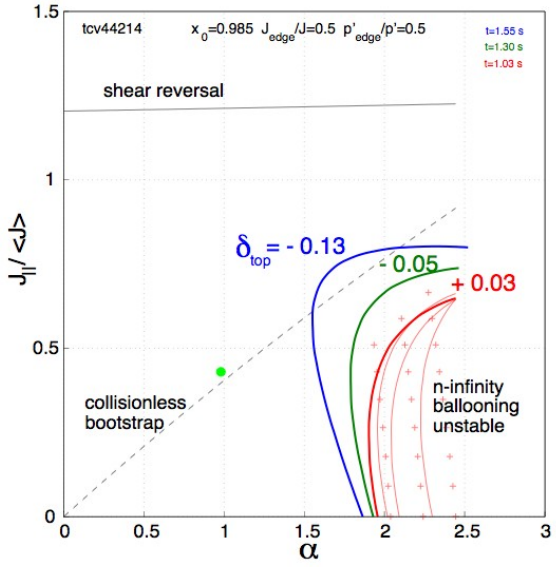

Fig.5.1 Triangularity δ_{top}-scan for SNC equilibria (see Fig.4.1), showing the shrinking and final disappearance of the accessible 2nd stability domain towards $\delta_{top}<0$. Thick lines show the ballooning limit at the maximum of pressure gradient in the pedestal. Red crosses and thin solid lines show the overall instability region taking into account all magnetic surfaces across the pedestal for $\delta_{top}=+0.03$.

In this diagram and in the experiment, this leads to a decrease of the edge pressure gradient and thus of the edge pressure pedestal (Fig.4.4), and hence of the ELM amplitude (Fig.4.3), both indeed found in the experiment. Note that the $n=\infty$ ballooning mode limit is the first limiting MHD which is a typical feature of the edge stability of negative triangularity equilibria [MedvEPS10, MedvEPS11]. More details on beta limits against global kink modes for different plasma profiles at negative triangularity are in [MedvEPS08].

These initial experiments in just one kind of equilibrium class with negative triangularity show already that negative triangularity H-mode with $\delta_{top}<0$ has the potential to mitigate ELMs and should therefore be further explored for a larger class of configurations involving negative triangularity.

For example, the effect of moving the X-point towards LFS is explored in a series of equilibria shown in Fig.5.2.a: The two first on the left have been operated in H-mode till $\delta_{top} \sim -0.25$. The 2nd enabled reliable H-mode operation (as described in above section 4), the 3rd was not yet developed to H-mode, the 4th is yet artificial. With the X-point moving to the LFS, stability calculations show that a region of "1st stability" at low values of $J_{||}$ develops to larger α. The higher edge shear as the X-points is moving to the LFS appear to open 1st stability region to higher pressures. Adding a further X-point to produce a double null divertor (DND) configuration reinforces this effect [MedvEPS11]. Since the experimental points in this diagram generally lay somewhat below the collisionless bootstrap line, these schemes enlarging the 1st stability region should be advantageous.

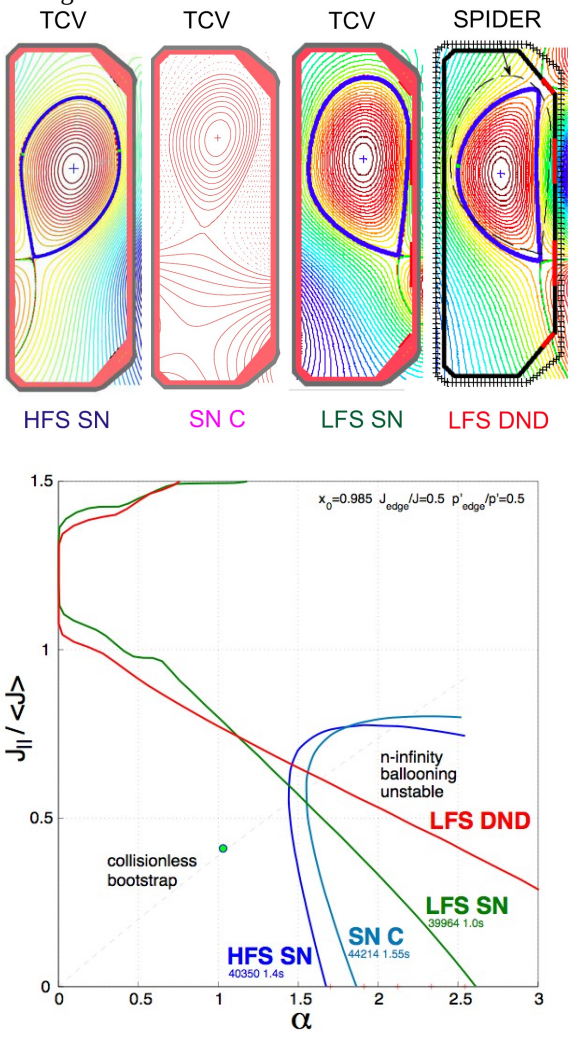

Fig.5.2 The displacement of the X-point major radius to larger values, keeping similar negative upper triangularity and elongation, opens progressively the low $J_{||}$ domain to larger pressure gradients.

The snowflake divertor concept was tested and developed for the first time in TCV [PirasPPCF09, PirasPPCF10] following the proposal by Ryutov [Ryutov08], and studied in H-mode in TCV [PirasPRL10]. The ELM characteristics changed from X-point to snowflake SF+ divertor, reducing the ELM frequency (×~0.3) and ELM average heat fluxes (×~0.4), although $\Delta W_{ELM}/W$ was found to increase (×~1.2-1.3) so far, probably linked to the higher pedestal stability (ideal

MHD) [PirasPRL10, Fig.5c]. Some part of the ELM characteristics changes here are unavoidably due to the inherent shape change, as the divertor goes from quadrupole to hexapole null.

Now, starting from a LFS SN, it is possible to substitute the X-point on the LFS by a snowflake, which further improves stability by further increasing the shear. A better stability figure results, substituting a snowflake (SF+) divertor to the LFS, by further increasing the edge shear. This further opens 1st stability to high α, and may be more significantly to higher $J_{\parallel}$ [MedveEPS11], as shown in Fig.5.3. This equilibrium is stable up to $\beta_N \sim 3$ for n=1-3 modes, and is compatible with TCV coil current requirements [Medvedev EPS11].

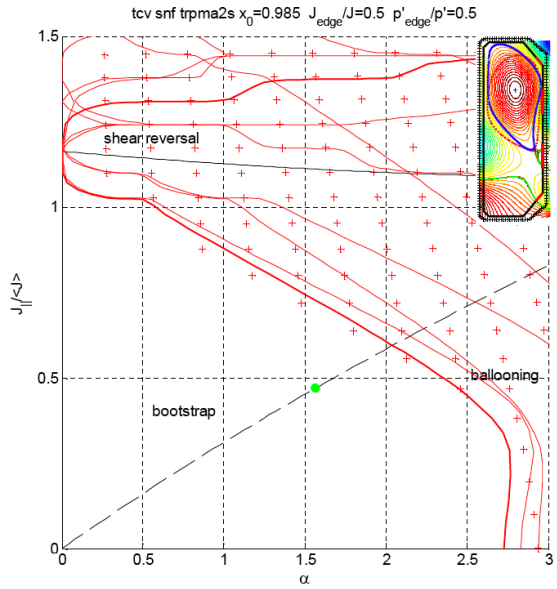

Fig.5.3 Snowflake on the LFS further increases the ballooning stable domain to higher $j_{\parallel}$, (LFS snowflake SF+, κ=2, δ_{top}=+0.5, δ_{bot}=-0.8).

Interestingly, a divertor configuration close to a moderately LFS snowflake was operated earlier in ELM-free H-mode in the DIII tokamak with controlled quasi-constant density (SF+, κ=1.9, δ_{top}=+0.3, δ_{bot}=-0.1), see Fig.1c in [Kameari87].

In summary, the initial experiments in TCV have demonstrated the potential to mitigate ELM heat losses by applying negative triangularity.

It would be of interest to develop these experiments in the direction of 1) a LFS divertor that advantageously increases the power damping surface ($\times 2\pi R$) and in the direction of 2) LFS snowflake divertor, which can distribute the conducted power to targets plate with 4 instead of 2 divertor legs and has in addition increased radiation volume due to the 2nd order null, while bearing promising stability properties.

5. Conclusions and outlook

The beneficial effect of negative triangularity was investigated at the level of energy confinement, radial heat transport from power balance, and to some initial part turbulence. Experiments reveal that the heat diffusivity is reduced to the core, although the geometric triangularity vanishes at the core. Similarly, the confinement response to a radial scan of power deposition shows major increase for δ<0, even on axis.

On the modelling side, *local* non-linear gyrokinetic simulations are explaining the effect of shape on heat diffusivity in terms of resonance tuning between the TEM and the TE precession frequency, different at the two triangularities. But they are unable to render the deep radial penetration of the transport modifications. *Global* gyrokinetic simulations in the TEM regime predict that the mixing length transport estimate improvement due to negative triangularity results from low-n TEM-modes of large radial extension. It is this radial extension, which by mediating core and edge, basically call for *global* transport analysis. The frequency of the low-n modes for which the global mixing length transport is modified with $\pm\delta$, corresponds to the frequencies for which turbulence amplitude changes are found in TCV.

Initial studies of H-mode with negative triangularity in single null centred discharges demonstrate dramatic mitigation of type I ELM peak power losses towards negative triangularity (factor 3 in the range -0.2 < δ_{top} < +0.2). This mitigation is obtained at the expense of a reduction of pedestal height.

Whether core confinement improvement towards negative triangularity can compensate the confinement loss at the pedestal depends on the turbulence regime. From the earlier experience, the collisionality in these TCV H-mode is rather on the high side to allow for clear core transport triangularity effects to develop, although in TEM dominated transport, a condition however possible in a reactor.

Summarizing for the reactor, and to our knowledge, to get the favourable effect of negative triangularity, are required: 1) low collisionality TEM regime, 2) global transport effects persisting at the higher ρ*-values of a reactor. The proper confinement regime(s) in the reactor is a matter of debate, although TEM turbulence dominated regime in presence of central electron α-heating is plausible. Whether these conditions will be

fulfilled in reactor plasma is not known yet, but such issue will soon be in the reach of HPC gyrokinetic calculations [Villars10].

Innovative candidate shapes with negative triangularity are proposed for exploration in TCV, including a LFS snowflake, or DND on the LFS, which by increasing the edge shear, increases substantially the edge pressure gradient in the 1st stability domain (after loosing the 2nd stability domain).

This work was supported in part by the Swiss National Science Foundation.

References

[1] F. Hofmann, et al., Plasma Phys. Control. Fusion **36**, B277 (1994).
[2] T.P. Goodman and the TCV Team, Nucl. Fus. **48**, 054011 (2008).
[3] A. Pochelon, T.P. Goodman, M.A. Henderson, et al., Nucl. Fusion **39**, 1807 (1999). A. Pochelon, S. Coda et al. 26th EPS Conf on Plasma Phys., ECA Vol. **23J**, P3.36 (1999).
[4] J-M. Moret et al., Phys. Rev. Lett. 79, 2057 (1997).
[5] Y. Camenen et al., Plasma Phys. Ctr. Fus **47**, 1971 (2005).
[6] Y. Camenen et al., Nucl. Fusion **47**, 510 (2007).
[7] A. Marinoni et al., Plasma Phys. Control. Fusion **51**, 055016 (2009).
[8] N. Kirneva et al., Plasma Phys. Control. Fusion **54**, 015011 (2012).
[9] S. Jolliet et al., Computer Phys. Comm. **177**, 409 (2007).
[10] S. Jolliet, Thesis EPFL no. 4326 (2009).
[11] B. Labit, A. Pochelon et al., Proc. IAEA FEC 2010 EXC/P8-08.
[12] A. Pochelon et al., 52nd APS DPP 2010, paper inv. N12.6.
[13] O. Sauter et al., Proc. IAEA FEC 2010 EXC/P8-16.
[14] J.-M. Moret, F. Buhlmann, and G. Tonetti, Review of Scientific Instruments **74**, 4634 (2003).
[15] J. Rossel, thesis EPFL, to appear (2012); Rossel et al., subm. to PRL.
[16] C. Angioni et al., Phys of Plasmas, **10**, 3225 (2003).
[17] L. Degtyarev et al. Comput. Phys. Commun. **103**, 10 (1997).
[18] S.Yu. Medvedev et al., Contrib. Plasma Phys. **50**, 324 (2010).
[19] S.Yu. Medvedev et al., 38th EPS Conf on Plasma Phys., P2.093 (2011).
[20] S.Yu. Medvedev, 37th EPS, ECA Vol.**34A** P4.145 (2010).
[21] S.Yu. Medvedev, 36th EPS, ECA Vol.**33E**, P2.143 (2009).
[22] S.Yu. Medvedev, 35th EPS, ECA Vol.**32D**, P1.072 (2008).
[23] F. Piras, et al., Plasma Phys. Control. Fusion **51**, 055009 (2009); F. Piras, et al., ibid. PPCF **52**, 124010 (2010).
[24] F. Piras, et al., Phys. Rev. Lett. **105**, 155003 (2010)
[25] D.D. Ryutov et al., Phys. Plasmas **15**, 092501 (2008).
[26] A. Kameari et al., Japan. J. of Appl. Phys. **26**, 598 (1987).
[27] L. Villard et al., Plasma Phys. Control. Fusion **52**, 124038 (2010).
[28] A. Pochelon, Y. Camenen, A. Marinoni et al., Proc. of 22nd IAEA Fusion Energy Conference, Geneva, Switzerland, 12-18 Oct 2008, EX/P5-15.